RESEARCH ARTICLE

Human Mutation

OFFICIAL JOURNAL
HGVS
HUMAN GENOME VARIATION SOCIETY
www.hgvs.org

Delineation of the Clinical, Molecular and Cellular Aspects of Novel *JAM3* Mutations Underlying the Autosomal Recessive Hemorrhagic Destruction of the Brain, Subependymal Calcification, and Congenital Cataracts

Nadia A. Akawi,[1] Fuat E. Canpolat,[2] Susan M. White,[3,4] Josep Quilis-Esquerra,[5] Martin Morales Sanchez,[5] Maria José Gamundi,[5] Ganeshwaran H. Mochida,[6] Christopher A. Walsh,[6] Bassam R. Ali,[1]* and Lihadh Al-Gazali[7]*

[1]Department of Pathology, Faculty of Medicine and Health Sciences, United Arab Emirates University, Al-Ain, United Arab Emirates; [2]Zekai Tahir Burak Maternity Hospital, Neonatal Intensive Care Unit, Ankara, Turkey; [3]Victorian Clinical Genetics Service, Murdoch Childrens Research Institute, Royal Children's Hospital, Australia; [4]Department of Paediatrics, University of Melbourne, Australia; [5]Molecular Genetics Unit. Consorci Sanitari de Terrassa, Terrassa, Barcelona, Spain; [6]Division of Genetics, Manton Center for Orphan Disease Research and Howard Hughes Medical Institute, Department of Medicine, Boston Children's Hospital, Boston, Massachusetts; [7]Department of Paediatrics, Faculty of Medicine and Health Sciences, United Arab Emirates University, Al-Ain, United Arab Emirates

Communicated by Segolène Ayme

Received 27 June 2012; accepted revised manuscript 5 December 2012.
Published online 15 December 2012 in Wiley Online Library (www.wiley.com/humanmutation). DOI: 10.1002/humu.22263

ABSTRACT: We have recently shown that the hemorrhagic destruction of the brain, subependymal, calcification, and congenital cataracts is caused by biallelic mutations in the gene encoding junctional adhesion molecule 3 (JAM3) protein. Affected members from three new families underwent detailed clinical examination including imaging of the brain. Affected individuals presented with a distinctive phenotype comprising hemorrhagic destruction of the brain, subependymal calcification, and congenital cataracts. All patients had a catastrophic clinical course resulting in death. Sequencing the coding exons of JAM3 revealed three novel homozygous mutations: c.2T>G (p.M1R), c.346G>A (p.E116K), and c.656G>A (p.C219Y). The p.M1R mutation affects the start codon and therefore is predicted to impair protein synthesis. Cellular studies showed that the p.C219Y mutation resulted in a significant retention of the mutated protein in the endoplasmic reticulum, suggesting a trafficking defect. The p.E116K mutant traffics normally to the plasma membrane as the wild-type and may have lost its function due to the lack of interaction with an interacting partner. Our data further support the importance of JAM3 in the development and function of the vascular system and the brain.

Hum Mutat 34:498–505, 2013. © 2012 Wiley Periodicals, Inc.

KEY WORDS: brain; subependymal calcification; congenital cataract; JAM3

Introduction

Junctional adhesion molecule 3 (JAM3; MIM #613730) is a member of the JAM subfamily of proteins, which include F11R (JAM1, JAM-A), JAM2 (JAM-B), JAM3 (JAM-C), and IGSF5 (JAM4) [Ebnet, 2008; Weber et al., 2007]. Other related members of this subfamily of proteins include endothelial cell selective adhesion molecule and coxasackie virus and adenovirus receptor (CXADR) [Weber et al., 2007]. JAMs and related proteins are localized at intercellular contacts and participate in the assembly and maintenance of tight junctions (TJs) and the control of cellular permeability [Ebnet, 2008]. TJs are morphologically distinct subcellular structures that are located closer to the apical side (compared with other junctional complexes) and are highly regulated areas of close contact between the plasma membranes of adjacent epithelial and endothelial cells [Balda and Matter, 2008]. TJs are important for the formation of polarized epithelial and endothelial barriers by forming intermembrane diffusion barriers and by controlling diffusion along the paracellular pathway [Cereijido et al., 2008]. It has also been found that TJs are important for intracellular signaling [Matter and Balda, 2007; Steed et al., 2009; Terry et al., 2010]. JAMs have been found to regulate adhesion between leukocytes and endothelial cells and the paracellular transmigration of leukocytes across the endothelium [Bradfield et al., 2007; Weber et al., 2007]. Moreover, JAMs play a role in cell polarization during spermatogenesis [Gliki et al., 2004].

In addition to JAMs, TJs contain other proteins including claudins, occludins, and tricellulins [Ebnet et al., 2004; Ebnet, 2008]. JAMs are single-span transmembrane proteins, whereas claudins, occludins, and tricellulins are tetraspan transmembrane proteins [Balda and Matter, 2008; Ebnet, 2008]. The tetraspan proteins form the paracellular permeability barrier and therefore determine the selectivity and extent of paracellular diffusion. JAMs on the contrary are postulated to mediate homotypic cell–cell adhesion [Bazzoni et al., 2000; Weber et al., 2007]. Several inherited conditions have been shown to be caused by mutations in genes encoding members of TJs protein complexes [O'Driscoll et al., 2010]. Hypomagnesemia has been shown to be caused by mutations in genes encoding claudins 16 and 19 [Konrad et al., 2006; Simon et al., 1999] and familial hypercholanemia to be caused by mutations in *TJP2* and

Additional Supporting Information may be found in the online version of this article.

*Correspondence to: Lihadh Al-Gazali, Department of Pediatrics, Faculty of Medicine and Health Sciences, United Arab Emirates University, P.O. Box 17666, Al-Ain, United Arab Emirates. E-mail: l.algazali@uaeu.ac.ae or Bassam R. Ali, Department of Pathology, Faculty of Medicine and Health Sciences, United Arab Emirates University, P.O. Box 17666, Al-Ain, United Arab Emirates. E-Mail: bassam.ali@uaeu.ac.ae, br_ali@hotmail.com

Contract grant sponsors: Dubai Harvard Foundation for Medical Research (DHFMR) (2008-04); United Arab Emirates PhD scholarships programme, National Institutes of Health (NINDS) (RO1 NS035129).

BAAT genes [Carlton et al., 2003]. Similarly, mutations in claudin 14 and tricellulin have been found to cause hereditary deafness [Riazuddin et al., 2006; Wilcox et al., 2001] and mutations in *NHS* to cause Nance-Horan syndrome [Burdon et al., 2003]. The variability in the clinical presentations reflects the variable functions of TJs in various tissues and organs.

We have recently identified a homozygous mutation in *JAM3* in a consanguineous family from the United Arab Emirates (UAE) with a rare recessive disorder that is characterized by hemorrhagic destruction of the brain, subependymal calcification, and congenital cataracts (MIM #613730) [Mochida et al., 2010]. In this manuscript, we describe three additional novel mutations in *JAM3* in patients from different ethnic backgrounds with similar phenotypes and elucidate the cellular mechanisms underlying some of those mutations.

Materials and Methods

Clinical Evaluations

All individuals participating in this study or their guardians provided written informed consents. Clinical assessments were performed by experienced clinical geneticists in Turkey, Spain, Australia, and the UAE. Full medical history was obtained. Participating members underwent careful clinical examination including imaging of the brain by magnetic resonance imaging (MRI).

Mutation Screening

Genomic DNA was extracted from peripheral leukocytes using the Flexigene DNA kit (Qiagen, Santa Clara, CA). Intronic primer pairs were designed to amplify individual *JAM3* exons and its exon/intron junctions using Primer3 (http://frodo.wi.mit.edu/). Following PCR amplification, the PCR products were cleaned using the ExoSAP-IT reagent (USB Co., Cleveland, OH) followed by DNA sequencing using the BigDye Terminator v3.1 Cycle Sequencing kit and run on an ABI PRISM 3130*xl* DNA Analyzer (Applied Biosystems, Foster City, CA). Sequencing data were analyzed using clustalw2 referencing the NCBI GeneBank NM_032801.4 for *JAM3* gene.

Site-Directed Mutagenesis

A transfection-ready *JAM3*-pCMV6 plasmid tagged C-terminally with Myc and Flag was purchased from OriGene Inc. (OriGene, Rockville, MD). The identified missense mutations (p.E116K and p.C219Y) were introduced by site-directed mutagenesis using *Pfu* Ultra high-fidelity DNA polymerase (Stratagene, La Jolla, CA) following the manufacturer's protocol. The primers used for site-directed mutagenesis are the following with the mutagenic nucleotide in bold:

(1) For generating c.346G>A (p.E116K) we used
Forward: 5′ CCCTTTATCGCTGT**A**AGGTCGTTGCTCG 3′
Reverse: 5′ CGAGCAACGACCT**T**ACAGCGATAAAGGG 3′
(2) For generating c.656G>A (p.C219Y) we used
Forward: 5′ CTGGGCAGTACTACT**A**CATTGCTTCCAATG 3′
Reverse: 5′ CATTGGAAGCAATG**T**AGTAGTACTGCCCAG 3′

All constructs were confirmed by DNA sequencing.

Cell Culture

Human cervical cancer (HeLa) cell lines were cultured in DMEM (Invitrogen, Carlsbad, CA) supplemented with 10% heat-inactivated fetal bovine serum at 37°C with 5% CO_2. Transient transfection of cells was achieved with FuGENE HD transfection reagent (Promega, Madison, WI) using 0.5 μg plasmid cDNA for confocal microscopy experiments. Cotransfection with hRas-GFP plasmid (0.2 μg cDNA) served as a transfection indicator and a plasma-membrane marker. All experiments were performed 24–48 hr following transfection.

Confocal Fluorescence Microscopy

Transfected cells were grown on coverslips (Ibidi, Martinsried, Germany) and fixed (5 min) with methanol (Sigma–Aldrich, St. Louis, MO) at –20°C. After three washes (5 min each) with PBS, cells were blocked with 1% BSA (Sigma–Aldrich) for 30 min. Membranes were incubated with primary antibodies at room temperature for 1 hr. Mouse antiflag (Sigma–Aldrich) and rabbit anticalnexin (Santa Cruz Biotechnology, Santa Cruz, CA) were used at 1:1,000 and 1:100 dilutions, respectively. After the primary antibodies incubations, the slides were washed three times (5 min each) then incubated for 1 hr at room temperature with secondary antibodies (fluorescence-labeled "Alexa-Fluor-568" [antimouse] and "Alexa-Fluor-488" [antirabbit]; Santa Cruz Biotechnology). Confocal microscopy was performed with a Nikon Eclipse system (Nikon Instruments Inc., Melville, NY). Control experiments without the primary antibodies or with nontransfected cells were carried out and revealed very low-level background staining.

Results

Clinical Features

Three families from different ethnic backgrounds (one Turkish, one Afghani, and one Moroccan) have been recruited to participate in this study (Fig. 1). Consanguinity is evident in two of the families and the clinical features of all the affected children are listed in Supp. Table S1.

Family 1: The parents of the affected child in this family are second cousins of Turkish origin. The parents are normal. Their first child (II1) was a preterm baby girl who had intracranial bleeding and died in the neonatal period. One of the mother's sisters died with similar phenotype but no clinical data were available. The second child (II2) of the couple was a female who was the product of normal pregnancy and term delivery. Her birth weight was 2,480 gm (<10th centile). She was admitted to the neonatal intensive care unit on day 5 because of the tonic seizures, which were resistant to treatment. Physical examination revealed a head circumference of 30 cm, sloping forehead, prominent, bulging anterior fontanelle, bitemporal grooving, and bilateral nuclear cataracts (Fig. 2A-1). Cranial ultrasound showed a prominent expansive bleeding. Brain computerized tomography showed calcification of the subependymal region and multifocal intraparenchymal hemorrhage (Fig. 2A-2). Serological tests were negative for toxoplasmosis, rubella, and cytomegalovirus. Cerebrospinal fluid PCR for cytomegalovirus and toxoplasma were also negative. Platelets levels were normal. The infant developed posthemorrhagic hydrocephalus and died at 2 months of age.

Family 2: The parents are nonconsanguineous and healthy of Afghani origin. Patient 1 (II1) was the first child of the family born at

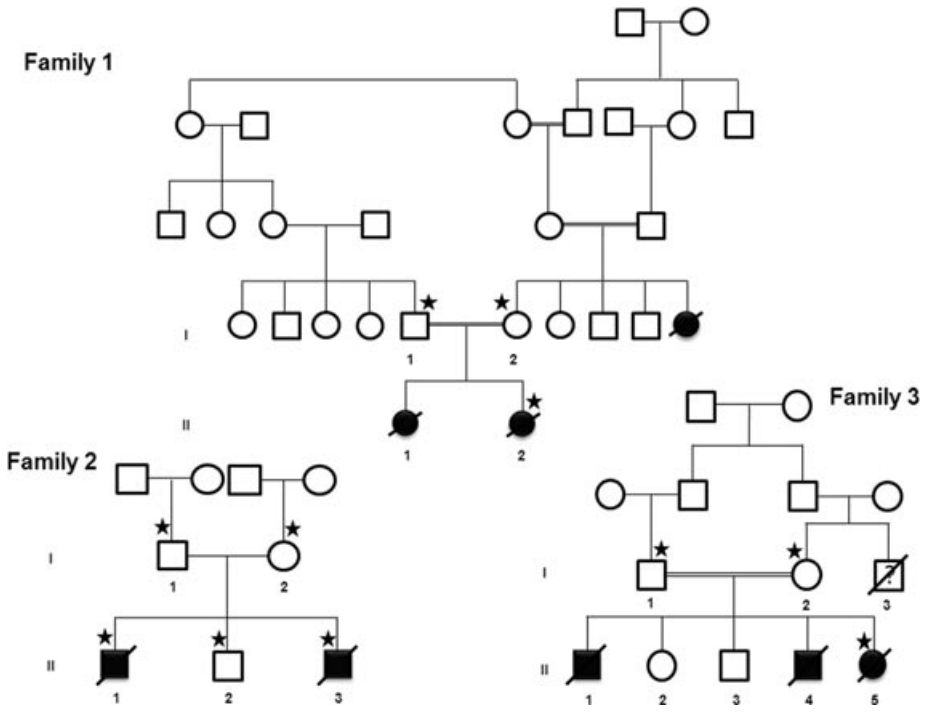

Figure 1. Pedigree drawings of the studied families. Three families with different ethnic origin were recruited in this study. Family 1 is Turkish, family 2 is Afghani, whereas family 3 is Moroccan. Filled symbols denote affected individuals with the syndrome of hemorrhagic destruction of the brain, subependymal calcification, and congenital cataracts. Sequenced individuals are indicated with an asterisk.

term by emergency caesarean section. His birth weight was 2,480 gm (<10th centile). He was noted to have bilateral cataracts and had feeding problems from birth. He was discharged home on day 4. At 2 weeks of age, he presented with vomiting, irritability, and a high-pitched cry. Brain MRI at the age of 15 days showed Grade IV intraventricular hemorrhage, severe ventricular dilatation, and white matter abnormalities in both cerebral hemispheres and multiple subependymal cysts (Fig. 2B). Renal ultrasound showed horseshoe kidneys with echogenic cortex and altered corticomedullary differentiation. He had progressive neurological deterioration and died at 2 weeks of age. Investigations were all normal and included respiratory chain enzymes on muscle and liver, 7 DHC, very long chain fatty acids, transferrin isoforms, blood karyotype, Affy 250K array, and coagulation study including platelets. Mitochondrial point mutations (MELAS, NARP, Leigh syndrome) were all negative.

Patient 2 (II3) was the third child of the family, with the family's second child being a healthy male. Patient 2's pregnancy was normal and delivery was by elective caesarean section at term. His birth weight was 3,315 gm (25th centile), length was 52 cm (50–90th centile), and head circumference was 35 cm (50th centile). At birth, he was noted to have bilateral cataracts. His tone and reflexes were normal and there was no clinical evidence of seizures. Cranial ultrasound showed periventricular echogenicity but there was no bleed. However, he deteriorated on day 5 and his hemoglobin dropped from 180 g/l to 96 d/l. He required ventilation. EEG on the third day of life showed bilateral epileptiform activity. Cranial ultrasound revealed extensive bilateral intracerebral hemorrhage. He died on the fifth day of life. Abdominal ultrasound showed pelvicalyceal dilatation of the right kidney. Full metabolic work up was normal.

Family 3: The parents are first cousins of Moroccan origin, who had a total of five pregnancies. The family history is significant in that the mother's brother (I3) died on the seventh day of life without any known diagnosis. This couple's first child was a male born at 36 weeks gestation who had cerebral hemorrhage, hydrocephalus, and died at 10 days of age. They then had two healthy children. The fourth pregnancy ended with a stillborn child who had hydrocephalus and the cerebral tissues showed necrotic degeneration. The index case (II5) is 28 days old female, the product of normal pregnancy. Fetal tachycardia was detected at 37 weeks gestation and therefore the baby was delivered by caesarean section. Her birth weight was 2,520 gm (10–25th centile), length 46.5 cm (25th centile), and head circumference 34.5 cm (50th centile). Bilateral cataracts were detected at birth both central and nuclear. On the second day of life, she presented with irritability, crying, and a bulging anterior fontanelle. Brain ultrasound showed dilated lateral ventricles, intraventricular hemorrhage in the right ventricle, and frontal periventricular cysts. On the eighth day of life, she was referred to another hospital for neurosurgical evaluation. Head CT revealed multifocal intraparenchymal hemorrhages, subependymal calcification, and diffusely hypodense brain parenchyma (Fig. 2C-1). MRI of the brain revealed intraventricular and intraparenchymal hemorrhage, edema, and cystic changes of the brain parenchyma, dilated ventricles, and thin corpus callosum with hemohrragic damage (Fig. 2C-2). There was normal circulation in the circle of Willis arteries. The EEG showed electrical status epilepticus, however, there were no seizures clinically. Metabolic screening was normal. Platelets levels were normal. It was decided that the child was not a candidate for ventricular shunt. She had severe anemia. Brain CT scan demonstrated bilateral subependymal calcification in the lateral ventricles. On the eighteenth day of life, her head circumference was 41 cm (+4 SD) and she was discharged for palliative care at home. She died at home the age of 39 days.

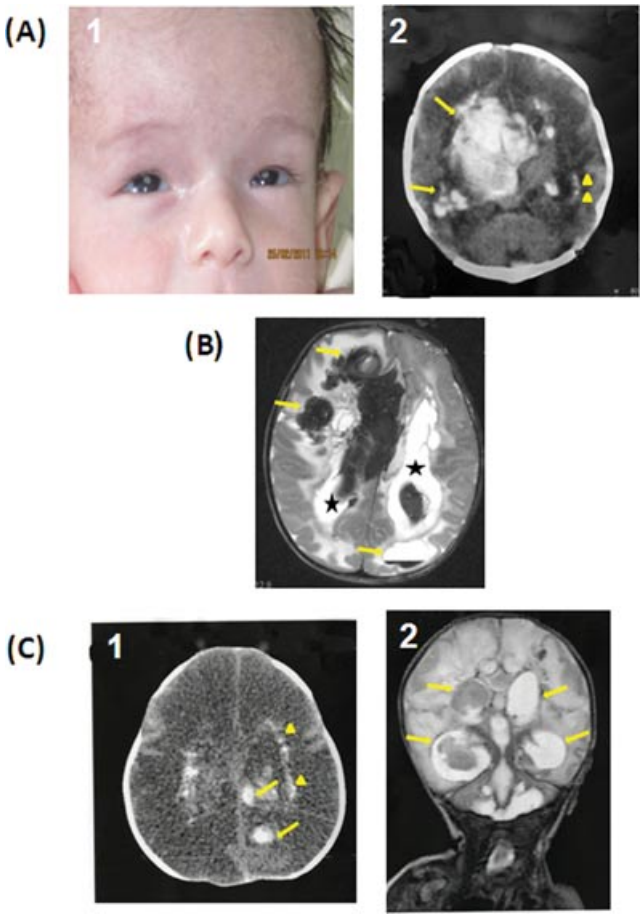

Figure 2. Clinical data. **A-1:** Facial picture of the affected individual in family 1 shows bilateral nuclear cataracts and hypertelorism. **A-2:** Head CT image of the patient in family 1 reveals multifocal intraparenchymal hemorrhages (arrows) and subependymal calcification (arrowheads). **B:** T2-weighted axial brain MRI of patient 1 in family 2 reveals multifocal intraparenchymal hemorrhages of varying ages (arrows) as well as intraventricular hemorrhage (asterisks). **C-1:** Head CT of the patient in family 3 shows multifocal intraparenchymal hemorrhages (arrows) and subependymal calcification (arrowheads). Diffusely hypodensity of brain parenchyma is also noted, suggesting severe edema. **C-2:** T2-weighted coronal MRI image of the same patient shows intraventricular hemorrhage with associated enlargement of the ventricles.

Mutation Analysis

DNA sequencing revealed three different homozygous missense mutations in *JAM3* gene in the three studied families (Table 1; Supp. Fig. S1). In family 1, we detected a nonsynonomous mutation (c.656G>A) in exon 6 of *JAM3* gene, which led to an amino acid substitution at position 219 (p.C219Y). In family 2, we identified a single nucleotide substituation (c.346G>A) in exon 4 of *JAM3* leading to a missense mutation at position 116 (p.E116K). The third mutation (c.2T>G) changed the initiator codon (methionine) of JAM3 leading to amino acid substitution to arginine (p.M1R). The three mutations were not reported in dbSNP or the 1000 genome project. All the amino acids affected by these mutations were highly conserved across species (Table 1) and were predicted to be disease causing by Polyphen2 (http://genetics.bwh.harvard.edu/pph2/), SIFT (http://sift.jcvi.org/), and Mutation taster (http://www.mutationtaster.org/). Furthermore, the detected mutations segregated with disease status in the three families; the parents were heterozygous, consistent with carrier status, and the available unaffected siblings were homozygous for the wild-type (WT) or heterozygous for the mutation. All the detected mutations were submitted to the LOVD database (www.lovd.nl/JAM3).

C219Y Mutation Results in JAM3 Trafficking Defect

To further understand the pathophysiological significance of the two detected missense mutations (p.E116K and p.C219Y), we employed confocal fluorescence microscopy to establish their subcellular localization relative to the WT-JAM3 protein. HeLa cells, known to lack endogenous expression of JAM3 [Betanzos et al., 2009], were either transfected with individual *JAM3* constructs (WT, p.E116K or p.C219Y) or cotransfected with GFP-hRas. The cells were then stained with antiflag antibodies to visualize *JAM3* constructs. The cells transfected with *JAM3* only constructs were costained with anticalnexin antibodies to visualize the endoplasmic reticulum (ER) network. As shown in panels A–F of Figure 3, the WT JAM3 is predominantly localized to the plasma membrane and colocalized largely with the GFP-hRas. Similarly, the p.E116K is predominantly localized to the plasma membrane as shown in panels G–L of Figure 3. On the contrary, the p.C219Y mutant colocalized predominantly with the ER marker (calnexin) and not with GFP-hRas indicating its retention in the ER (Fig. 3, panels M–R, Supp. Fig. S2).

Discussion

The Impact of JAM3 Mutations on the Protein Product

Arrate et al. (2001) and Santoso et al. (2002) cloned and characterized JAM3 as an approximately 43 kDa transmembrane glycoprotein. This type I integral membrane glycoprotein consists of two immunoglobulin (Ig)-like domains with intrachain disulfide bonds at the extracellular region. By sequence analysis, Arrate et al. (2001) concluded that the N-terminal domain is a V-type, whereas the membrane proximal domain is a C2-type. Also they predicted that the intrachain disulfide bonds that stabilize each Ig domain are between C53–C115 and C160–C219. Ig-like domains are implicated in a range of vital functions, including cell–cell recognition, cell-surface receptors, muscle structure, and the immune system [Teichmann and Chothia, 2000]. The C-terminal region of the protein is composed of a short transmembrane domain followed by an intracellular domain containing a PDZ binding motif (Supp. Fig. S1A).

The p.C219Y mutation detected in family 1 alters one of the four highly conserved cysteine residues of JAM3 disrupting one out of two disulfide bonds known to stabilize the Ig-folds of the protein [Arrate et al., 2001; Santoso et al., 2002]. Several functional studies demonstrated that cysteine-substitutions disrupt the structure of cell surface proteins causing their misfolding, instability, and ER retention [Fukuda et al., 2011; Rudarakanchana et al., 2002]. In consistent, comparison of the subcellular localization of flag-tagged C219Y mutants transiently expressed in HeLa (Fig. 3; Supp. Fig. S2A) and COS7 (Supp. Fig. S2C) clearly showed that most of the mutated protein failed to reach the cell membrane. ER retention is a well established disease causing mechanism in many human syndromes caused by loss-of-function mutations [Aridor, 2007; Ali et al., 2010; 2011; Chen et al., 2005].

The p.E116K mutation found in family 2 did not seem to affect the subcellular localization or trafficking of the protein (Fig. 3). However, its position in the Ig-like V-type domain suggests an interfering role of this mutation with the dimerization or with the

Table 1. Mutations Detected in *JAM3*

Exon	cDNA change[a]	Protein change[a]	Genotype	Mutation type	Domain	Conservation[c]	Likelihood of pathogenicity	References
5	c.612+1G>T (c.747+1G>T)[b]	p.V205L*fs* (p.V250L*fs*X26)[b]	Homozygous	Splice site	C-terminus	Normal CAGGCACTTTGGTAAGATCTCTTC Mutated CAGGCACTTTGTTAAGATCTCTTC Human CAGGCACTTTGGTAAGATCTCTTC Chimp CAGGCACTCTGGTAAGATCTCTT Cat GGCACTCTGGTAAGATCTCTT Mouse CAGGCACTCTGGTAAGA	19 bp insertion leads to a frame shift and created premature termination codon	Mochida et al. (2010)
6	c.656G>A	p.C219Y	Homozygous	Nonsynonomous	Ig-like C2-type	Normal FTAVHKDDSGQYYCIASNDAGSARCEE Mutated FTAVHKDDSGQYYYIASNDAGSARCEE G.gallus FHAVHKGDTGRYSCIATNDAGFAKCEE M.musculus FNAVHKDDSGQYYCIASNDAGAARCEG R.norvegicus FSAVHKEDSGQYYCIASNDAGAARCEG C.lupus FSAVHKEDSGQYYCIASNDAGSARCEE B.taurus FSAVHKEDSGQYYCIASNDAGSARCEE H.sapiens FTAVHKDDSGQYYCIASNDAGSARCEE P.troglodytes FTAVHKDDSGQYYCIASNDAGSARCEE D.rerio FSAVRKEDAGEYYCRAKNEAGISECGP D.rerio FRSVKKEDAGEYYCQARNEAGWSKCIR	Misfolding of the protein leads to its retention in the endoplasmic reticulum	This article
4	c.346G>A	p.E116K	Homozygous	Nonsynonomous	Ig-like V-type	Normal TRRDSALYRCEVVARNDRKEIDEIVIE Mutated TRRDSALYRCKVVARNDRKEIDEIVIE G.gallus TRMDTATYRCEVAAPSDTKTIDEINIQ M.musculus TRSDSAIYRCEVVALNDRKEVDEITIE R.norvegicus TRSDSAIYRCEVVALNDRKEVDELTIE C.lupus TRTDSALYRCEVVARNDRKEIDEIVIE B.taurus TRKDSALYRCEVVARNDRKEIDEIVIE H.sapiens TRRDSALYRCEVVARNDRKEIDEIVIE P.troglodytes TRRDSALYRCEVVARNDRKEIDEIVIE D.rerio TRSDSADYRCEVTAPNDQKSFDEILIS D.rerio SRSDTAQYRCEVAAIDDQKPFDEILIS	Protein–protein interactions defects	This article
1	c.2T>G	p.M1R	Homozygous	Nonsynonomous	N-terminus	Normal MALRRPPRLRLCARLPDFFLLLLFRGC Mutated RALRRPPRLRLCARLPDFFLLLLFRGC G.gallus ----------MSCAISYSLLFVFPGC M.musculus MALSRRLRLRLYARLPDFFLLLLFRGC R.norvegicus MALSRRLRLRLCARLPDFFLLLLFRGC C.lupus FESVE---------------MAVLQGC B.taurus MALRRRPSLVL--------LLLLVRGC H.sapiens MALRRPPRLRLCARLPDFFLLLLFRGC P.troglodytes MALRRPPRLRLCARLPDFFLLLLFRGC D.rerio TEHFTDSKMALTPLACVLLLLSMQCYI D.rerio --------MAFGRQTLSLVLFYWLCNS	Translation aberrations leading to loss or abnormal expression	This article

[a]Mutation nomenclature is based on NM_032801.4 and NP_116190.3 starting from A of the ATG as 1.
[b]The nomenclature used by Mochida et al. (2010) based on NM_032801.3.
[c]Conservation alignments for all the missense mutations are based on homoloGene results for JAM3 (ID: 83700), but the splice site mutation alignments were adopted from Mutationtaster (http://www.mutationtaster.org/) results.

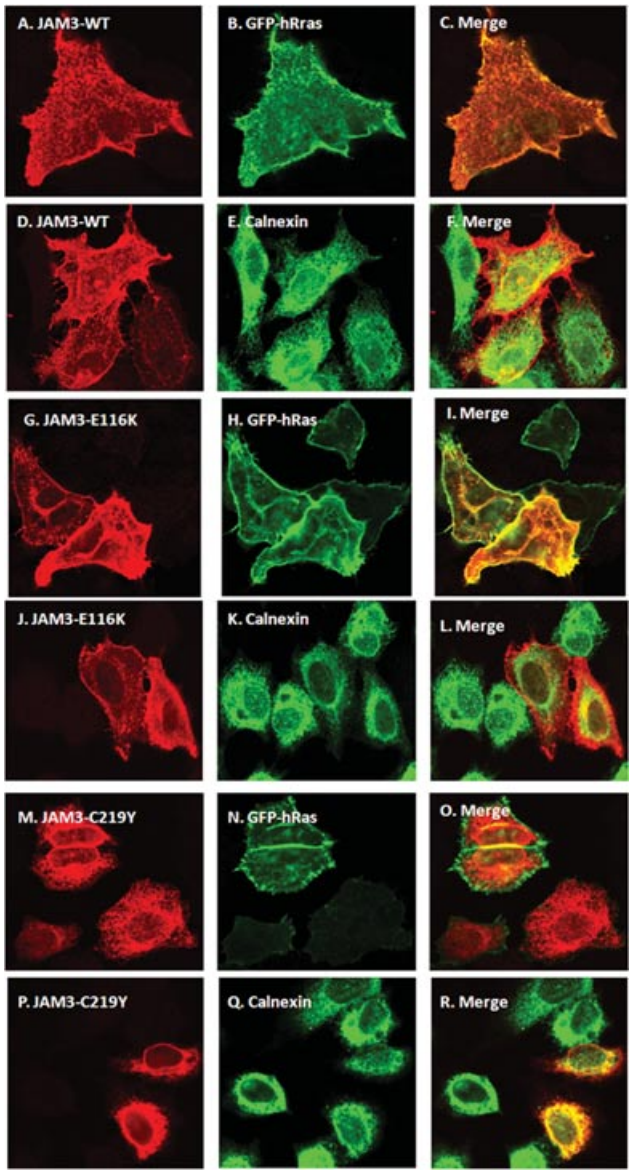

Figure 3. p.C219Y mutation disrupts normal intracellular JAM3 protein localization. HeLa cells transiently transfected with C-terminal flag-tagged *JAM3*-pCMV5 vector constructs wild type (WT), **A–F**; p.E116K, **G–L**; and p.C219Y, **M–R**) and stained with antiflag Ab (red). WT vector localizes to the plasma membrane (PM) with the hRas-GFP-tagged marker (**A–C**) and not with the endoplasmic reticulum (ER) marker calnexin (green; **D–F**). JAM3–p.E116K–flag construct localization was similar to the WT with hRas-GFP-tagged marker (**G–I**) and the calnexin (**J–L**). p.C219Y construct do not localize at the PM-like hRas-GFP-tagged marker (**M–O**) and appears to be accumulated or clustered within the ER with calnexin (**P–R**).

interaction(s) of this protein with one or more of its interacting partners. JAM3 controls TJ maintenance by engaging in homophilic and heterophilic interactions with neighboring JAM molecules [Ebnet et al., 2008].

Arrate et al. (2001) and Santoso et al. (2002) predicted the first ATG by homology alignments between *JAM3*, *JAM1*, *JAM2*, and mouse *Jam3*. Arrate et al. (2001) found using SignalP V1.1 the signal sequence of JAM3, which should be cleaved after glycine 30 from the putative ATG. The mutated methionine in family 3 is predicted to be the first methionine of JAM3 protein and such mutations almost invariably interfere with the translation of the protein. However, there are two in-frame ATG's upstream of this start codon and the improbable use of one of them or for the next in-frame ATG would encode a non-functional or unstable protein.

Clinical Consequences of JAM3 Deficiency

Mouse Jam3 is expressed at the apical junctions of endothelial cells, smooth muscle cells, fibroblasts, Schwann cells, spermatids, and hematopoietic stem cells. More recently, Jam3 expression was detected in the TJs of neural stem cells in the embryonic ventricular zone and the adult ependymal cell layer of mouse brain [Stelzer et al., 2012]. More than half of mice with homozygous mutation in *Jam3* exhibit postnatal lethality. *Jam3* deficient mice exhibit growth retardation, muscle weakness, abnormal spermatogenesis, granulocytes homeostasis defects, electrophysiological defects, and hypersensitivity to mechanical stimuli [Colom et al., 2012; Scheiermann et al., 2007]. Furthermore, mouse Jam3 apical expression was found on the embryonic retinal neuroepithelia, and its deficiency caused nuclear congenital cataracts [Daniele et al., 2007]. The brains of mice lacking Jam3 are abnormal in some strains [Wyss et al., 2012] but relatively unaffected in others [Stelzer et al., 2012].

In humans, Mochida et al. (2010) demonstrated that a homozygous mutation in *JAM3* is the cause of a severe autosomal recessive syndrome segregating in a consanguineous family. The affected members in this family were born with congenital cataracts and developed severe brain abnormalities from progressive hemorrhagic destruction of the brain tissue, including the cerebral white matter and basal ganglia. Three out of six affected individuals died early in infancy. Brain imaging in all the affected showed calcification in the subependymal region of the brain, multifocal intraparenchymal hemorrhage with associated liquefaction, and massive cystic degeneration resulting in large ventricles [Al-Gazali et al., 1999; Mochida et al., 2010]. The phenotype of the children in this report is very similar to the phenotype of the affected children in this previously reported family. All the affected children in this report had bilateral cataracts and develop progressive neurological impairment, associated with seizures in some individuals. In addition neuroimaging in all patients showed intraparanchymal hemorrhage with evidence of brain destruction and subependymal, basal ganglia, and white matter calcification. These changes are very similar to those found in the original family. Some of the other features described in the original family, such as renal anomalies and liver enlargement, were more variable in this patient group. All the affected children in this report died. Therefore, of the total 10 cases reported so far the disorder was lethal in 7 cases. Death occurred in the first few weeks of life. Those who survived (three in total) are severely retarded with severe spasticity and seizures.

Other conditions that could be considered in the differential diagnosis include the syndrome of band-like intracranial calcification, simplified cerebral gyrai, and polymicrogyria [Abdel-Salam et al., 2008; O'Driscoll et al., 2010]. This syndrome is caused by mutations in another TJ gene, occludin (*OCLN*; MIM #602876). However, patients with this syndrome do not have intracranial hemorrhage or congenital cataract [Mochida et al., 2010]. Furthermore, our patients did not show any evidence of developmental malformation of the cerebral cortex and polymicrogyria. Similarly mutations in collagen type IV alpha (*COL4A1*; MIM #120130) can cause overlapping clinical presentations, which include antenatal intracranial hemorrhage [de Vries et al., 2009], brain small vessel disease with hemorrhage or vascular leukoencephalopathy, porencephaly [Gould et al., 2006; Sibon et al., 2007], and hereditary angiopathy with nephropathy, aneurysms, and muscle cramps [Plaisier et al.,

2007]. All these disorders are inherited as autosomal dominant and the clinical presentations is different from the cases in this report. Proliferative vasculopathy and hydranencephaly–hydrocephaly syndrome (Fowler syndrome) is an autosomal recessive perinatally lethal disorder characterized by hydrocephalus associated with progressive destruction of the central nervous system (CNS) tissue as a result of an unusual and characteristic proliferative vasculopathy [Fowler et al., 1973]. The hallmark of the syndrome is the microvascular proliferation, which is associated with extensive necrosis and calcification of the CNS tissue. There are no visceral malformations [Lalonde et al., 2010]. It is caused by mutations in the *FLVCR2* gene (MIM #610865). Clinically affected fetuses present with fetal akinesia deformation sequence with muscular neurogenic atrophy [Fowler et al., 1973; Meyer et al., 2010], which is different from the clinical presentation of the cases in this report.

Our study revealed several missense mutations scattered throughout the coding sequence of *JAM3* affecting different domains yet the affected children shared similar phenotype indicating homogeneity of this disorder at the clinical and molecular level. This is likely due to the total loss of the protein function as a result of those mutations.

Conclusions

Our study confirms the importance of JAM3 as a component of the junctional complexes and its deficiency leading to a distinctive and catastrophic neonatal presentation of cataracts and hemorrhagic destruction of the brain.

Acknowledgments

We are grateful to the participating families and clinicians. We thank Davinia VAZQUEZ SANCHEZ, Ramon VIDAL SANAHUJA in Hospital de Tarrasa (Barcelona) for their help. We thank Dr. A. James Barkovich for his help in interpreting brain imaging studies. C.A.W. is an Investigator of the Howard Hughes Medical Institute.

Disclosure statement: The authors declare no conflict of interest.

References

Abdel-Salam GM, Zaki MS, Saleem SN, Gaber KR. 2008. Microcephaly, malformation of brain development and intracranial calcification in sibs: pseudo-TORCH or a new syndrome. Am J Med Genet 146A:2929–2936.

Al-Gazali LI, Sztriha L, Dawodu A, Varady E, Bakir M, Khdir A, Johansen J. 1999 Complex consanguinity associated with short rib-polydactyly syndrome III and congenital infection-like syndrome: a diagnostic problem in dysmorphic syndromes. J Med Genet 36:461–466.

Ali BR, Ben-Rebeh I, John A, Akawi NA, Milhem RM, Al-Shehhi NA, Al-Ameri MM, Al-Shamisi SA, Al-Gazali L. 2011. Endoplasmic reticulum quality control is involved in the mechanism of endoglin-mediated hereditary haemorrhagic telangiectasia. PLoS One 6:e26206.

Ali BR, Xu H, Akawi NA, John A, Karuvantevida NS, Langer R, Al-Gazali L, Leitinger B. 2010. Trafficking defects and loss of ligand binding are the underlying causes of all reported DDR2 missense mutations found in SMED-SL patients. Hum Mol Genet 19:2239–2250.

Aridor M. 2007. Visiting the ER: the endoplasmic reticulum as a target for therapeutics in traffic related diseases. Adv Drug Deliv Rev 59:759–781.

Arrate MP, Rodriguez JM, Tran TT, Brock TA, Cunningham SA. 2001. Cloning of human junctional adhesion molecule 3 (JAM3) and its identification as the JAM2 counter-receptor. J Biol Chem 276:45826–45832.

Balda MS, Matter K. 2008. Tight junctions at a glance. J Cell Sci 121:3677–3682.

Bazzoni G, Martinez-Estrada OM, Orsenigo F, Cordenonsi M, Citi S, Dejana E. 2000. Interaction of junctional adhesion molecule with the tight junction components ZO-1, cingulin, and occludin. J Biol Chem 275:20520–20526.

Betanzos A, Schnoor M, Severson EA, Liang TW, Parkos CA. 2009. Evidence for cross-reactivity of JAM-C antibodies: implications for cellular localization studies. Biol Cell 101:441–453.

Bradfield PF, Nourshargh S, Aurrand-Lions M, Imhof BA. 2007 JAM family and related proteins in leukocyte migration (Vestweber series). Arterioscler Thromb Vasc Biol 27:2104–2112.

Burdon KP, McKay JD, Sale MM, Russell-Eggitt IM, Mackey DA, Wirth MG, Elder JE, Nicoll A, Clarke MP, FitzGerald LM. 2003. Mutations in a novel gene, NHS, cause the pleiotropic effects of Nance-Horan syndrome, including severe congenital cataract, dental anomalies, and mental retardation. Am J Hum Genet 73:1120–1130.

Carlton VE, Harris BZ, Puffenberger EG, Batta AK, Knisely AS, Robinson DL, Strauss KA, Shneider BL, Lim WA, Salen G. 2003. Complex inheritance of familial hypercholanemia with associated mutations in TJP2 and BAAT. Nat Genet 34:91–96.

Cereijido M, Contreras RG, Shoshani L, Flores-Benitez D, Larre I. 2008. Tight junction and polarity interaction in the transporting epithelial phenotype. Biochim Biophys Acta 1778:770–793.

Chen Y, Bellamy WP, Seabra MC, Field MC, Ali BR. 2005. ER-associated protein degradation is a common mechanism underpinning numerous monogenic diseases including Robinow syndrome. Hum Mol Genet 4:2559–2569.

Colom B, Poitelon Y, Huang W, Woodfin A, Averill S, Del Carro U, Zambroni D, Brain SD, Perretti M, Ahluwalia A, Priestley JV, Chavakis T, et al. 2012. Schwann cell-specific JAM-C-deficient mice reveal novel expression and functions for JAM-C in peripheral nerves. FASEB J 26:1064–1076.

Daniele LL, Adams RH, Durante DE, Pugh EN Jr, Philp NJ. 2007. Novel distribution of junctional adhesion molecule-C in the neural retina and retinal pigment epithelium. J Comp Neurol 505:166–176.

de Vries LS, Koopman C, Groenendaal F, Van Schooneveld M, Verheijen FW, Verbeek E, Witkamp TD, van der Worp HB, Mancini G. 2009. COL4A1 mutation in two preterm siblings with antenatal onset of parenchymalhemorrhage. Ann Neurol 65:12–18.

Ebnet K. 2008. Organization of multiprotein complexes at cell–cell junctions. Histochem Cell Biol 130:1–20.

Ebnet K, Suzuki A, Ohno S, Vestweber D. 2004. Junctional adhesion molecules (JAMs): more molecules with dual functions? J Cell Sci 117:19–29.

Fowler M, Dow R, White TA, Greer CH. 1972. Congenital hydrocephalus-hydrencephaly in five siblings, with autopsy studies: a new disease. Dev Med Child Neurol 14:173–88.

Fukuda Y, Aguilar-Bryan L, Vaxillaire M, Dechaume A, Wang Y, Dean M, Moitra K, Bryan J, Schuetz JD. 2011. Conserved intramolecular disulfide bond is critical to trafficking and fate of ATP-binding cassette (ABC) transporters ABCB6 and sulfonylurea receptor 1 (SUR1)/ABCC8. J Biol Chem 286:8481–92.

Gliki G, Ebnet K, Aurrand-Lions M, Imhof BA, Adams RH. 2004. Spermatid differentiation requires the assembly of a cell polarity complex downstream of junctional adhesion molecule-C. Nature 431:320–324.

Gould DB, Phalan FC, van Mil SE, Sundberg JP, Vahedi K, Massin P, Bousser MG, Heutink P, Miner JH, Tournier-Lasserve E, John SW. 2006. Role of COL4A1 in small-vessel disease and hemorrhagic stroke. N Engl J Med 354:1489–1496.

Konrad M, Schaller A, Seelow D, Pandey AV, Waldegger S, Lesslauer A, Vitzthum H, Suzuki Y, Luk JM, Becker C, Schlingmann KP, Schmid M, et al. 2006. Mutations in the tight-junction gene claudin 19 (CLDN19) are associated with renal magnesium wasting, renal failure, and severe ocular involvement. Am J Hum Genet 79:949–957.

Lalonde E, Albrecht S, Ha KC, Jacob K, Bolduc N, Polychronakos C, Dechelotte P, Majewski J, Jabado N. 2010. Unexpected allelic heterogeneity and spectrum of mutations in Fowler syndrome revealed by next-generation exome sequencing. Hum Mutat 31:918–923.

Matter K, Balda MS. 2007. Tight junctions, gene expression and nucleo-junctinal interplay. J Cell Sci 120:1505–1511.

Meyer E, Ricketts C, Morgan NV, Morris MR, Pasha S, Tee LJ, Rahman F, Bazin A, Bessières B, Déchelotte P, Yacoubi MT, Al-Adnani, et al. 2010. Mutations in FLVCR2 are associated with proliferative vasculopathy and hydranencephaly-hydrocephaly syndrome (Fowler syndrome). Am J Hum Genet 86:471–478.

Mochida GH, Ganesh VS, Felie JM, Gleason D, Hill RS, Clapham KR, Rakiec D, Tan WH, Akawi N, Al-Saffar M, Partlow JN, Tinschert S, et al. 2010. A homozygous mutation in the tight-junction protein JAM3 causes hemorrhagic destruction of the brain, subependymal calcification, and congenital cataracts. Am J Hum Genet 87:882–889.

O'Driscoll MC, Daly SB, Urquhart JE, Black GC, Pilz DT, Brockmann K, McEntagart M, Abdel-Salam G, Zaki M, Wolf NI, Ladda RL, Sell S, et al. 2010. Recessive mutations in the gene encoding the tight junction protein occludin cause band-like calcification with simplified gyration and polymicrogyria. Am J Hum Genet 87:354–364.

Plaisier E, Gribouval O, Alamowitch S, Mougenot B, Prost C, Verpont MC, Marro B, Desmettre T, Cohen SY, Roullet E, Dracon M, Fardeau M, et al. 2007. COL4A1 mutations and hereditary angiopathy, nephropathy, aneurysms, and muscle cramps. N Engl J Med 357:2687–2695.

Riazuddin S, Ahmed ZM, Fanning AS, Lagziel A, Kitajiri S, Ramzan K, Khan SN, Chattaraj P, Friedman PL, Anderson JM. 2006. Tricellulin is a tight-junction protein necessary for hearing. Am J Hum Genet 79:1040–1051.

Rudarakanchana N, Flanagan JA, Chen H, Upton PD, Machado R, Patel D, Trembath RC, Morrell NW. 2002. Functional analysis of bone morphogenetic protein type II receptor mutations underlying primary pulmonary hypertension. Hum Mol Genet 11:1517–1525.

Santoso S, Sachs UJH, Kroll H, Linder M, Ruf A, Preissner KT, Chavakis T. 2002. The junctional adhesion molecule 3 (JAM-3) on human platelets is a counterreceptor for the leukocyte integrin Mac-1. J Exp Med 196:679–691.

Scheiermann C, Meda P, Aurrand-Lions M, Madani R, Yiangou Y, Coffey P, Salt TE, Ducrest-Gay D, Caille D, Howell O, Reynolds R, Lobrinus A, et al. 2007. Expression and function of junctional adhesion molecule-C in myelinated peripheral nerves. Science 318:1472–1475.

Sibon I, Coupry I, Menegon P, Bouchet JP, Gorry P, Burgelin I, Calvas P, Orignac I, Dousset V, Lacombe D, Orgogozo JM, Arveiler B, et al. 2007. COL4A1 mutation in Axenfeld-Rieger anomaly with leukoencephalopathy and stroke. Ann Neurol 62:177–184.

Simon DB, Lu Y, Choate KA, Velazquez H, Al-Sabban E, Praga M, Casari G, Bettinelli A, Colussi G, Rodriguez-Soriano J, McCredie D, Milford D, et al. 1999. Paracellin-1, a renal tight junction protein required for paracellular Mg^{2+} resorption. Science 285:103–106.

Steed E, Balda MS, Matter K. 2010. Dynamics and functions of tight junctions. Trends Cell Biol 20:142–149.

Stelzer S, Worlitzer MM, Bahnassawy L, Hemmer K, Rugani K, Werthschulte I, Schön AL, Brinkmann BF, Bunk EC, Palm T, Ebnet K, Schwamborn JC. 2012. JAM-C is an apical surface marker for neural stem cells. Stem Cells Dev 21:757–66.

Teichmann SA, Chothia C. 2000. Immunoglobulin superfamily proteins in *Caenorhabditis elegans*. J Mol Biol 296:1367–1383.

Terry S, Nie M, Matter K, Balda MS. 2010. Rho signaling and tight junction functions. Physiology (Bethesda) 25:16–26.

Weber C, Fraemohs L, Dejana E. 2007. The role of junctional adhesion molecules in vascular inflammation. Nat Rev Immunol 7:467–477.

Wilcox ER, Burton QL, Naz S, Riazuddin S, Smith TN, Ploplis B, Belyantseva I, Ben-Yosef T, Liburd NA, Morell RJ. 2001. Mutations in the gene encoding tight junction claudin-14 cause autosomal recessive deafness DFNB29. Cell 104:165–172.

Wyss L, Schäfer J, Liebner S, Mittelbronn M, Deutsch U, Enzmann G, Adams RH, Aurrand-Lions M, Plate KH, Imhof BA, Engelhardt B. 2012. Junctional adhesion molecule (JAM)-C deficient C57BL/6 mice develop a severe hydrocephalus. PLoS One 7:e45619.